BONE REMODELING IN RESPONSE TO A NEW BIOMIMETIC POLYMER-COMPOSITE HIP STEM: COMPUTATIONAL STUDY USING MECHANO-BIOCHEMICAL MODEL

Pouria Tavakkoli Avval[a], Saeid Samiezadeh[a], Habiba Bougherara[a*]

[a] *Department of Mechanical and Industrial Engineering, Ryerson University, 350 Victoria Street, Toronto, Ontario, Canada, M5B 2K3*
** habiba.bougherara@ryerson.ca*

Keywords: biomimetic composite, hip stem, bone remodeling, total hip arthroplasty, mechano-biochemical model.

Abstract

Periprosthetic bone loss following total hip arthroplasty (THA) is a serious concern leading to the premature failure of implant. Based on Wolff's law, a stiff prosthesis induces a huge bone loss at the vicinity of the implant. Therefore, designing flexible implants and investigating its effect on bone remodeling process is of paramount for the purpose of developing long lasting prosthesis. In this study, bone remodeling around a relatively new biomimetic polymer composite-based (CF/PA12) hip implant was compared to that in a metallic one (made from Titanium) using the mechano-biochemical bone adaptation model (irreversible thermodynamic-based model). The results revealed that the composite stem results in fewer density changes (bone loss) compared to Titanium one. The amount of bone loss predicted with the Ti stem was approximately 21% which is greater than that found in the presence of the CF/PA12 stem (i.e. 9%).

1. Introduction

Periprosthetic bone loss following total hip arthroplasty (THA) is a serious concern leading to the premature failure of implants. The uneven load sharing between the implant and the bone is believed as one of the main causes of bone loss (stress shielding phenomenon) [1]. According to the Wolff's law, the reduction of mechanical stress causes bone to adapt itself by reducing its mass, either by getting thinner (external remodeling) or by becoming more porous (internal remodeling) [1].

Stress shielding phenomenon is attributed to implant design [2, 3] and pre-operative bone quality [4, 5]. Nowadays, composite materials are attractive for the implantation purposes as they can withstand high stresses while provide flexible structure [6, 7]. Since it is not always feasible to follow-up the long-term behavior of the bone after implantation, it is important to develop realistic models to predict the bone evolution and thus monitor bone loss. In this investigation, a mechano-biochemical model (thermodynamic-based model) which considers a coupling between the mechanical loading and biochemical affinity of reactions as a stimulus for bone remodeling [8-10] was used to predict the bone density distribution around a biomimetic hip stem made from polymer composites (carbon fiber polyamide 12: CF/PA12) [11].

2. Materials and methods

2.1. Mechano-biochemical model

In the mechano-biochemical model (thermodynamic-based model), bone is considered as an open thermodynamic system that exchanges matter and energy with its surrounding. All biochemical reactions describing the mechanism of bone remodeling (i.e. formation of multinucleated osteoclasts, old bone decomposition, production of osteoblast activator, osteoid production, and calcification) obey the general form of Menten-Michaelis enzyme reaction [12]. The thermodynamic model was validated in previous studies [8-10]. The equations governing the bone remodeling process were developed based on the coupling between mechanical and biochemical fluxes or forces. In order to include the mechanical effects onto the biochemical reactions, the standard law of mass action was modified as follows:

$$r_\alpha = l_{\alpha\alpha} A_\alpha + l_{\alpha\upsilon} d_{(1)} = k_{+\alpha} \prod_{i=1}^{n} \left[N_i\right]^{\upsilon_{\alpha i}} - k_{-\alpha} \prod_{i=1}^{n} \left[N_i\right]^{\upsilon'_{\alpha i}} + l_{\alpha\upsilon} d_{(1)} \qquad (1)$$

where the rate and affinity of the α^{th} biochemical reaction are denoted by r_α and A_α, respectively. Phenomenological and reaction rate coefficients are shown by l_{ij} and $k_{\pm j}$, respectively. $d_{(1)}$ stands for the first invariant of the strain rate tensor representing the rate of volume change. $\upsilon_{\alpha i}$ and $\upsilon'_{\alpha i}$ are the stoichiometric coefficients of substance N_i entering and leaving the α^{th} reaction, respectively. And, the concentration of substance N_i is denoted by $\left[N_i\right]$.

Using the modified version of the law of mass action, a system of differential equations (governing the bone remodeling mechanism) was derived. These equations yielded the time evolution of concentration of substances participating in the biochemical reactions of bone remodeling. The solution of these equations was expressed in terms of the reaction rate, the initial concentration and flux of substances as well as the effect of mechanical load on the biochemical reactions. All model parameters can be found in [10].

The bone density (ρ) was related to the initial bone density (ρ_0), the normalized concentration of old bone ($\overline{[Old\_B]}$) and new bone ($\overline{[New\_B]}$) according to:

$$\rho = \rho_0 \cdot \left(\overline{[Old\_B]} + \overline{[New\_B]}\right) \qquad (2)$$

Using the empirical power law relationship provided by Carter and Hayes [13], the modulus of elasticity of the bone was calculated by:

$$E = \left[E_{Old\_B} \cdot \left(\frac{\overline{[Old\_B]}}{\overline{[Old\_B]} + \overline{[New\_B]}} \right) + E_{New\_B} \cdot \left(\frac{\overline{[New\_B]}}{\overline{[Old\_B]} + \overline{[New\_B]}} \right) \right] \left(\frac{\rho}{\rho_0} \right)^2 \qquad (3)$$

where E_{New_B} and E_{Old_B} represent the elastic modulus of new and old bone, respectively.

2.2. CAD models and finite element analysis (FEA)

The CAD model of large left 4th generation composite femur (model 3406, sawbones, Vashon, WA, USA) was imported into SolidWorks software (SolidWorks Corp., Dassualt Systèmes, Concord, MA, USA) for the purpose of virtual implantation (details are provided in our previous work [10]). The CAD model of hip stem was also developed by commercially available software (CATIA V5R13, Dassault systemes, Montreal, CA).

In order to obtain the bone density distribution throughout the intact femur, the prepared CAD model was imported into ANSYS (ANSYS Inc., Canonsburg, Pennsylvania, USA). In the first iteration of the numerical simulation, the inner (cancellous) and outer (cortical) layers were modeled as homogenous structures with an initial density of 0.98 gr/cm^3 (ρ_0) which represents an average value of cortical bone with 1.64 gr/cm^3 and cancellous bone with 0.32 gr/cm^3. To model the intact femur, the material properties of cortical were assigned to the outer layer of the femur [14]. Furthermore, the inner layer, and the hip implant were considered to consist of cancellous bone with properties taken from [14]. In the next iterations, the new properties of each element were calculated based on the concentration of *Old* and *New* bones remained/produced inside the element.

The bone and the internal polymeric core of the implant were meshed by ten-node higher order three dimensional (3D) tetrahedral solid elements (SOLID187), whereas, the composite layers (laminate) were meshed using SHELL181 elements. The contacts between all surfaces were considered to be perfectly bonded similar to [1, 15]. All the interfaces were also meshed by CONTA174 and TARGE170.

In order to simulate the physiological loading, muscle and hip joint reaction forces regarding 45% of gait cycle were applied to the models [16, 17]. To avoid any stress concentration, muscle and hip joint reaction forces were distributed over several nodes of greater (and lesser) trochanter and femoral head, respectively. To avoid rigid body motion, the degrees of freedom of all nodes at the distal femur were fixed (Figure 1).

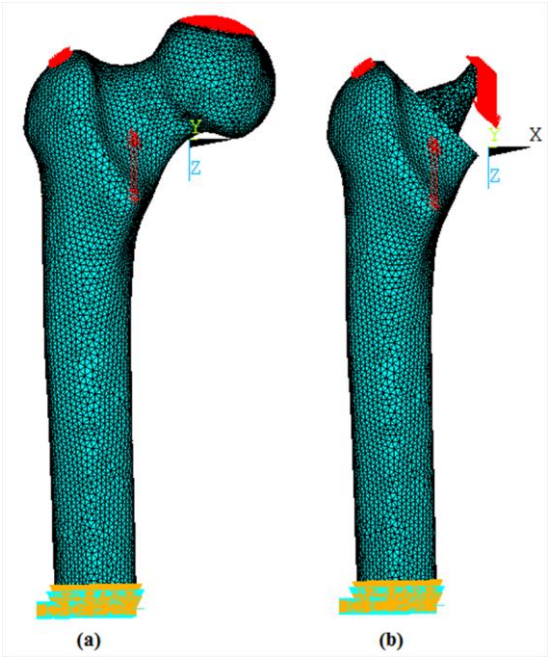

Figure 1. Location of loads and constraints applied on the models.

The thermodynamic-based model was applied to the meshed model in ANSYS Parametric Design Language (APDL). FEA yielded the trace of the strain tensor to calculate the values of *Old* and *New* bone concentrations for each element. The density and modulus of elasticity of each element were then obtained by using Eqs. (2) and (3), respectively. The new material properties were used for the next iteration, and the process was repeated until no significant change in the density of the elements was observed (further details can be found in our previous works [8, 10]).

To simulate bone remodeling in response to THA, the elements of the femoral head (and neck) of the intact femur were removed (unselected). The material properties of hip implant (Titanium or composite) were assigned to the hip implant. The initial material properties of each element of immediate post-operative femur were chosen from the same element in the post convergence-intact femur. The joint reaction force was also transferred to the hip implant head. Finally, the mechano-biochemical model (thermodynamic-based model) and convergence criteria were applied again.

It should be mentioned that the composite hip stem was composed of a 3 mm thick substructure made of several layers of CF/PA12 and an internal polymeric core with the Young's modulus and Poisson's ratio of 1 GPa and 0.2, respectively [11, 18]. The material properties of CF/PA12 are listed in Table 1 and were assigned to the hip implant by ACP (Pre) module of ANSYS Workbench 14.5. The stacking sequence of the composite was $(\pm 45^{o})_{6}$.

Material Properties	Value/Type
E_L	66.5 GPa
E_T	2.72 GPa
G_{LL}	19.5 GPa
G_{LT}	2.7 GPa
ν_{LL}	0.04
ν_{LT}	0.26
Ply Type	Woven

Table 1. Material properties of CF/PA12 lamina.

The metallic hip stem was made of Ti6Al4V with the Young's modulus and Poisson's ratio of 114 GPa and 0.3, respectively [19].

3. Results and Discussion

3.1. Pre-operative bone density distribution

Bone density distribution throughout the intact femur obtained by using the thermodynamic-based model is illustrated in Figure 2. The range of bone density varies between 0.35 and 1.75 gr/cm^3 which agrees with clinical observations [20, 21].

The maximum value of the bone density was observed in the outer cortex at mid-shaft region. In addition, dense trabecula was found in the region between the location of hip joint reaction force and the calcar. Similarly, such a dense cancellous bone carrying the stress from the superior contact surface to the calcar region of the medial cortex was observed in the study conducted by Kuhl and Balle [15].

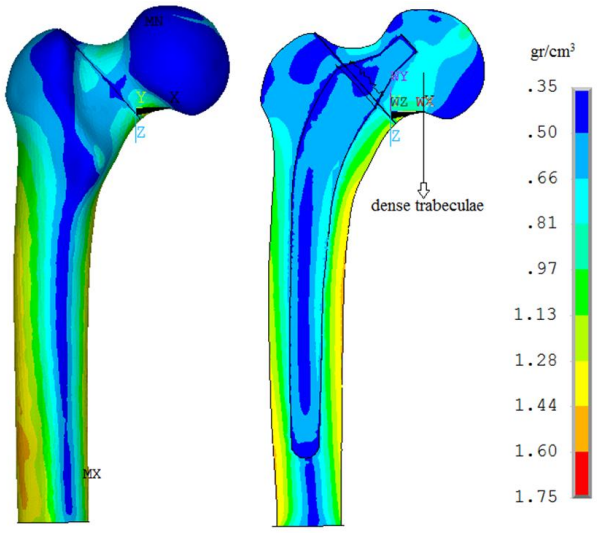

Figure 2. Density distribution in the intact femur obtained by the thermodynamic-based model.

3.2. Percent change in the bone density

Figure 3 demonstrates the percent change of femoral density in response to THA using both Titanium and composite hip implants. In both scenarios, the maximum periprosthetic bone loss was observed in the calcar region which is consistent with clinical observations [22]. Furthermore, the maximum bone formation was seen in the distal region of the hip stem which is due to the distal load transfer from the stem to the bone.

As illustrated in Figure 3, the stiffness of the hip implant plays a key role in the periprosthetic bone density distribution. It can be seen that the range of bone loss in the lateral/medial regions of the femur in response to Titanium hip implant (25% to 40%) was greater than that resulted from a composite one (10% to 25%). The amount of bone loss predicted with the Titanium stem was approximately 21% which is greater than that found with CF/PA12 stem (i.e. 9%). These results agree with the fact that more flexible implants provide less stress shielding.

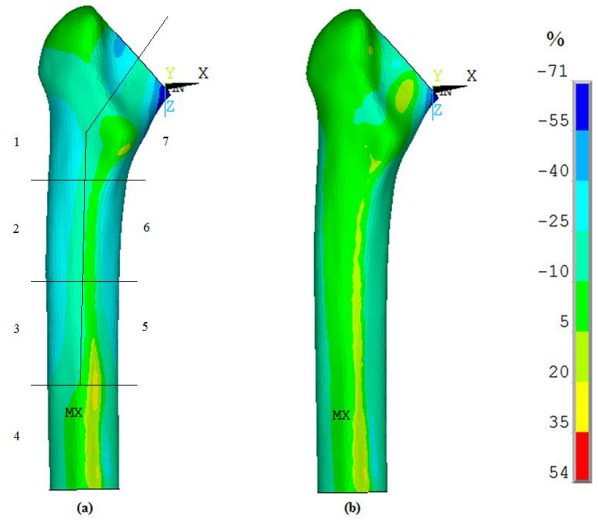

Figure 3. Percent change of femoral density in the presence of (a) Titanium (b) composite hip implant.

Table 2 shows the femoral density changes at the vicinity of the composite hip implant (Gruen zones [23]). It reveals that periprosthetic bone loss induced by the composite prosthesis (the flexible stem) is approximately the same (~ 10%) in all Gruen zones which is similar to Huiskes et al. [1] study using a flexible hip stem with the material properties of cortical bone.

Zone #	Bone loss %
1	8.6
2	9.8
3	10.5
4	8.7
5	9.7
6	9.5
7	9.7

Table 2. Periprosthetic bone loss induced by the composite hip implant.

3.3. Limitations of the study

Although the results agreed well with the bone morphology and literature, the model has some limitations and simplifications. Firstly, the concept of coupling is based on linear non-equilibrium thermodynamics and thus is phenomenological. Therefore, we cannot relate it directly to actual mechanosensing or mechanotransduction processes in cells. Secondly, in the simulations, the mechanical stimuli do not include any viscous effects. Thirdly, we disregarded kinetics of some of the known control mechanisms in bone remodeling such as the RANKL-RANK-OPG chain. Fourthly, in the proposed model the computational steps are unrelated to real time. However, the convergence of the iterative process was assumed when no significant change in the density of the elements was observed which is considered as the long-term response, from the clinical point of view.

4. Conclusions

The results of bone remodeling simulations revealed that CF/PA12 composite stem results in fewer density changes (bone loss) compared to Titanium made stem. This shows the benefits of composite-based stems in reducing the negative effect of stress shielding phenomena which is likely to reduce future periprosthetic fracture.

References

[1] R. Huiskes, H. Weinans, B. van Rietbergen. The relationship between stress shielding and bone resorption around total hip stem and the effects of flexible materials. *Clin Orthop Relat Res*, 274 124–134, 1992.

[2] J. D. Bobyn, A. H. Glassman, H. Goto, J. J. Krygier, J. E. Miller, C. E. Brooks. The effect of stem stiffness on femoral bone resorption after canine porous-coated total hip arthroplasty. *Clin Orthop Relat Res*, (261):196-213, 1990.

[3] D. R. Sumner, J. O. Galante. Determinants of stress shielding: design versus materials versus interface. *Clin Orthop Relat Res*, (274):202-212, 1992.

[4] C. A. Engh, J. P. Hooten, K. F. Zettl-Schaffer, M. Ghaffarpour, McGovern, T.F., G. E. Macalino, B. A. Zicat. Porous-coated total hip replacement. *Clin Orthop Relat Res*, 298:89–96, 1994.

[5] C. A. Engh, T. F. McGovern, J. D. Bobyn, W. H. Harris. A quantitative evaluation of periprosthetic bone-remodeling after cementless total hip arthroplasty. *J Bone Joint Surg Am*, 74(7):1009-1020, 1992.
[6] Z. S. Bagheri, I. El Sawi, E. H. Schemitsch, R. Zdero, H. Bougherara. Biomechanical properties of an advanced new carbon/flax/epoxy composite material for bone plate applications. *Journal of the Mechanical Behavior of Biomedical Materials*, 20(0):398-406, 2013.
[7] F. S. Siddiqui, S. Shah, B. Nicayenzi, E. H. Schemitsch, R. Zdero, H. Bougherara. Biomechanical analysis using infrared thermography of a traditional metal plate versus a carbon fibre/epoxy plate for Vancouver B1 femur fractures. *Proceedings of the Institution of Mechanical Engineers, Part H: Journal of Engineering in Medicine*, 228(1):107-113, 2014.
[8] H. Bougherara, V. Klika, F. Marsik, I. A. Marik, L. Yahia. New predictive model for monitoring bone remodeling. *J Biomed Mater Res A*, 95(1):9-24, 2010.
[9] V. Klika, F. Marsik. A thermodynamic model of bone remodelling: the influence of dynamic loading together with biochemical control. *J Musculoskelet Neuronal Interact*, 10(3):220-230, 2010.
[10] P. Tavakkoli Avval, V. Klika, H. Bougherara. Predicting bone remodeling in response to total hip arthroplasty: Computational study using mechano-biochemical model. *J Biomech Eng*, 2014, DOI: 10.1115/1.4026642.
[11] H. Bougherara, M. Bureau, M. Campbell, A. Vadean, L. Yahia. Design of a biomimetic polymer-composite hip prosthesis. *J Biomed Mater Res A*, 82(1):27-40, 2007.
[12] L. Michaelis, M. L. Menten. Kinetik der invertinwirkung. *Biochem Z*, 49:333–369, 1913.
[13] D. R. Carter, W. C. Hayes. The compressive behavior of bone as a two-phase porous structure. *J Bone Joint Surg Am*, 59(7):954-962, 1977.
[14] Sawbones Worlwide. Composite bone. 2013; Online document. Available from: http://www.sawbones.com/products/bio/composite.aspx.
[15] E. Kuhl, F. Balle. Computational modeling of hip replacement surgery: total hip replacement vs hip resurfacing. *Technische mechanik* 25(2):107–114, 2005.
[16] R. A. Brand, D. R. Pedersen, D. T. Davy, G. M. Kotzar, K. G. Heiple, V. M. Goldberg. Comparison of hip force calculations and measurements in the same patient. *J Arthroplasty*, 9(1):45-51, 1994.
[17] G. N. Duda, M. Heller, J. Albinger, O. Schulz, E. Schneider, L. Claes. Influence of muscle forces on femoral strain distribution. *J Biomech*, 31(9):841-846, 1998.
[18] H. Bougherara, M. N. Bureau, L. Yahia. Bone remodeling in a new biomimetic polymer-composite hip stem. *J Biomed Mater Res A*, 92(1):164-174, 2010.
[19] A. W. Turner, R. M. Gillies, R. Sekel, P. Morris, W. Bruce, W. R. Walsh. Computational bone remodelling simulations and comparisons with DEXA results. *J Orthop Res*, 23(4):705-712, 2005.
[20] R. Hodgskinson, J. D. Currey. The effect of variation in structure on the Young's modulus of cancellous bone: a comparison of human and non-human material. *Proc Inst Mech Eng H*, 204(2):115-121, 1990.
[21] M. Hoiberg, T. L. Nielsen, K. Wraae, B. Abrahamsen, C. Hagen, M. Andersen, et al. Population-based reference values for bone mineral density in young men. *Osteoporos Int*, 18(11):1507-1514, 2007.
[22] T. Niinimaki, P. Jalovaara. Bone loss from the proximal femur after arthroplasty with an isoelastic femoral stem. BMD measurements in 25 patients after 9 years. *Acta Orthop Scand*, 66(4):347-351, 1995.
[23] T. A. Gruen, G. M. McNeice, H. C. Amstutz. Modes of failures of cemented stem-type femoral components. *Clin Orthop Relat Res*, 141:17–27, 1979.